Comparison of Energy Based Hysteresis Models

Manfred Kaltenbacher[1], Klaus Roppert[1], Lukas Daniel Domenig[1], and Herbert Egger[2]
[1]Institute of Fundamentals and Theory in Electrical Engineering, TU Graz, Austria
[2]Institute for Computational Mathematics, Johannes Kepler University Linz, Austria

Energy based (EB) hysteresis models are thermodynamic consistent, show high potential for physically modeling ferromagnetic materials with high precision and have the capability to be implemented in Finite Element (FE) formulations with high efficiency. In this contribution, we review two EB hysteresis models and show their equivalence analytically. Furthermore, we provide details of the parameter identification based on Epstein frame measurements and an efficient Finite Element (FE) formulation. Finally, we demonstrate the applicability and numerical efficiency of the vector hysteresis model to rotating magnetic fields.

Index Terms—**Energy based vector hysteresis, Finite element analysis.**

I. Introduction

In [1], the vector generalization of the Jiles-Atherton (JA) model has been revisited and by applying fundamental ideas stated in [2] an energy-consistent vector hysteresis model for ferromagnetic materials could be obtained. In [3], a formulation being variational consistent, so that all internal variables follow from the minimization of a thermodynamic potential has been proposed. A further energy based variational model is presented in [4] together with an efficient numerical scheme, avoiding the usually employed approximation leading to inaccurate results in the vectorial case. Here, we review the two hysteresis models of [3] and [4] and establish their equivalence theoretically. In addition, we discuss our parameter identification scheme based on Epstein frame measurement and the efficient Finite Element (FE) formulation based on a quasi-Newton method. Finally, we provide numerical computations of a ferromagnetic material in a rotating magnetic field.

II. Analysis of Energy Based Hysteresis Models

The standard relation for ferromagnetic materials reads as

$$\boldsymbol{b} = \mu_0\big(\boldsymbol{h} + \boldsymbol{m}\big) = \mu_0\boldsymbol{h} + \boldsymbol{j}_{\mathrm{m}} \tag{1}$$

with the permeability of free space μ_0, magnetic flux density $\boldsymbol{b}$, magnetic field strength $\boldsymbol{h}$, magnetization $\boldsymbol{m}$ and magnetic polarization $\boldsymbol{j}_{\mathrm{m}}$. Thereby, the energy density may be written as

$$w(\boldsymbol{h},\boldsymbol{m}) = \frac{\mu_0}{2}|\boldsymbol{h}|^2 + e(\boldsymbol{m}), \tag{2}$$

with $e(\boldsymbol{m})$ the internal energy determined by the magnetization $\boldsymbol{m}$. The total change of w computes by (a dot denotes the time derivative)

$$\begin{aligned}\frac{d}{dt}w(\boldsymbol{h},\boldsymbol{m}) &= \mu_0\boldsymbol{h}\cdot\left(\tfrac{1}{\mu_0}\dot{\boldsymbol{b}} - \dot{\boldsymbol{m}}\right) + \tfrac{\partial e}{\partial \boldsymbol{m}}(\boldsymbol{m})\cdot\dot{\boldsymbol{m}}\\ &= \boldsymbol{h}\cdot\dot{\boldsymbol{b}} - \left(\mu_0\boldsymbol{h} - \tfrac{\partial e}{\partial \boldsymbol{m}}(\boldsymbol{m})\right)\cdot\dot{\boldsymbol{m}}\,.\end{aligned} \tag{3}$$

Via the following definitions

$$\boldsymbol{h}_{\mathrm{r}} := \tfrac{1}{\mu_0}\tfrac{\partial e}{\partial \boldsymbol{m}}(\boldsymbol{m}) \quad \text{and} \quad \boldsymbol{h}_{\mathrm{i}} := \boldsymbol{h} - \boldsymbol{h}_{\mathrm{r}}, \tag{4}$$

Manuscript received February 1, 2022; revised March 28, 2022. Corresponding author: M. Kaltenbacher (email: manfred.kaltenbacher@tugraz.at).

the total magnetic field strength $\boldsymbol{h}$ is split into a *reversible* part $\boldsymbol{h}_{\mathrm{r}}$ and an *irreversible* part $\boldsymbol{h}_{\mathrm{i}}$. Thereby, (3) may be written as

$$\frac{d}{dt}w(\boldsymbol{b},\boldsymbol{m}) = \boldsymbol{h}\cdot\dot{\boldsymbol{b}} - \mu_0\boldsymbol{h}_{\mathrm{i}}\cdot\dot{\boldsymbol{m}}\,, \tag{5}$$

which corresponds to the thermodynamic principle that the change of energy is equal to the sum of the change of work and dissipation. To ensure an appropriate dissipation behavior, the irreversible field is postulated to satisfy (5) by

$$\mu_0\boldsymbol{h}_{\mathrm{i}}\cdot\dot{\boldsymbol{m}} = \chi|\dot{\boldsymbol{m}}|\,, \tag{6}$$

which describes the work delivered by the pinning force (opposing the motion of Bloch walls) with χ denoting the magnitude of the pinning force.

Both publications [3] as well as [4] then us a pseudo time-stepping and replace $\dot{\boldsymbol{m}}$ by $\boldsymbol{m} - \boldsymbol{m}_{\mathrm{p}}$, where $\boldsymbol{m}_{\mathrm{p}}$ is the value of magnetization from the previous time step. The constitutive model in [3] is based on a variational principle, namely

$$\boldsymbol{m} = \arg\min_{\boldsymbol{m}} e(\boldsymbol{m}) - \mu_0\langle\boldsymbol{h},\boldsymbol{m}\rangle + \chi|\boldsymbol{m} - \boldsymbol{m}_{\mathrm{p}}|\,, \tag{7}$$

with $\langle\cdot,\cdot\rangle$ denoting the Euclidean inner product. Assuming e to be strictly convex, this uniquely describes $\boldsymbol{m}$ as a function of $\boldsymbol{h}$ and $\boldsymbol{m}_{\mathrm{p}}$. Alternatively, in [4], the following constitutive equation is proposed

$$\boldsymbol{h}_{\mathrm{r}} = \arg\min_{\boldsymbol{u}\in K(\boldsymbol{h})} S(\boldsymbol{u}) - \langle\boldsymbol{m}_{\mathrm{p}},\boldsymbol{u}\rangle, \tag{8}$$

with $S(\boldsymbol{u})$ defined as the Legendre-Fenchel conjugate function of $(1/\mu_0)\partial e/\partial\boldsymbol{m}$. Hence

$$\frac{\partial S}{\partial \boldsymbol{u}}(\boldsymbol{h}_{\mathrm{r}}) = \boldsymbol{m} \quad \Leftrightarrow \quad \boldsymbol{h}_{\mathrm{r}} = \frac{1}{\mu_0}\frac{\partial e}{\partial \boldsymbol{m}}(\boldsymbol{m}). \tag{9}$$

The set $K(\boldsymbol{h})$ over which is minimized is given by

$$K(\boldsymbol{h}) = \{\boldsymbol{u} : |\boldsymbol{u} - \boldsymbol{h}| \le \chi\}\,. \tag{10}$$

Both models are motivated by an analogy with mechanics, i.e., a model for dry friction, as outlined in [5]. In the following, we briefly recall this model and interpret the magnetic quantities accordingly. Following [5], a dry friction model is based on a space V of velocities $\boldsymbol{v}$, the dual space $F = V'$ of forces $\boldsymbol{f}$, and a closed convex and non-empty subset C of *admissible* *velocities*. The relation between $\boldsymbol{v}$ and $\boldsymbol{f}$ is then specified by the maximum-dissipation principle

$$\max_{\boldsymbol{f}\in C}(-\langle \boldsymbol{v},\boldsymbol{f}\rangle) = \max_{\boldsymbol{f}}(-\langle \boldsymbol{v},\boldsymbol{f}\rangle + \psi_C(\boldsymbol{f}))\,, \qquad (11)$$

where ψ_C is the indicator function of the subset C defined by

$$\psi_C(\boldsymbol{f}) = \begin{cases} 0 & \text{if } \boldsymbol{f}\in C \\ \infty & \text{if } \boldsymbol{f}\notin C \end{cases} . \qquad (12)$$

Please note that the minus sign in (11) comes from the opposite directions of $\boldsymbol{f}$ and $\boldsymbol{v}$ to model friction. The first order optimality condition for the problem can be stated as

$$-\boldsymbol{v}\in\partial\psi_C(\boldsymbol{f}) \qquad (13)$$

with $\partial\psi_C$ denoting the sub-differential of the indicator function ψ_C. Alternatively, the relation coupling $\boldsymbol{f}$ and $\boldsymbol{v}$ can be characterized by the dual problem

$$\boldsymbol{f}\in\partial\psi_C^*(-\boldsymbol{v})\,, \qquad (14)$$

where ψ_C^* is the Legendre-Fenchel conjugate function of ψ_C.

In the context of magnetic hysteresis, the velocity and force correspond to the rate of the magnetization $\dot{\boldsymbol{m}}$ and the irreversible magnetic field intensity $\boldsymbol{h}_\mathrm{i}$

$$\boldsymbol{v} = -\dot{\boldsymbol{m}} \qquad \text{and} \qquad \boldsymbol{f} = \boldsymbol{h}_\mathrm{i}\,. \qquad (15)$$

The dissipated power thus is given by

$$-\langle \boldsymbol{f},\boldsymbol{v}\rangle = \mu_0\boldsymbol{h}_\mathrm{i}\cdot\dot{\boldsymbol{m}}\,, \qquad (16)$$

in perfect correspondence with the energy dissipation identity (5).

Let us now draw the connection to the two constitutive models introduced in [3], [4]. Using the indicator function, the variational problem (8) can be written equivalently as

$$\begin{aligned}\boldsymbol{h}_\mathrm{r} = \boldsymbol{h}-\boldsymbol{h}_\mathrm{i} &= \arg\max_{\boldsymbol{u}\in K} S(\boldsymbol{h}-\boldsymbol{u}) - \langle \boldsymbol{m}_\mathrm{p}, \boldsymbol{h}-\boldsymbol{u}\rangle \qquad (17)\\ &= \arg\max_{\boldsymbol{u}} S(\boldsymbol{h}-\boldsymbol{u}) - \langle \boldsymbol{m}_\mathrm{p}, \boldsymbol{h}-\boldsymbol{u}\rangle + \psi_K(\boldsymbol{u}),\end{aligned}$$

where $K = \{\boldsymbol{u} : |\boldsymbol{u}| \le \chi\}$ denotes the set of admissible irreversible fields $\boldsymbol{h}_\mathrm{i}$. The first order optimality condition for this problem reads

$$\tfrac{\partial S}{\partial \boldsymbol{u}}(\boldsymbol{h}_\mathrm{r}) - \boldsymbol{m}_\mathrm{p} \in \partial\psi_K(\boldsymbol{h}_\mathrm{i}). \qquad (18)$$

Using the definition $\boldsymbol{m} = \frac{\partial S}{\partial \boldsymbol{u}}(\boldsymbol{h}_\mathrm{r})$ as well as $-\boldsymbol{v} = \boldsymbol{m} - \boldsymbol{m}_\mathrm{p}$ and $\boldsymbol{f} = \boldsymbol{h}_\mathrm{i}$, this exactly amounts to (13) with convex set $C = K$. We now turn to the model (7) and observe that $\chi|\boldsymbol{m}-\boldsymbol{m}_\mathrm{p}| = \psi_K^*(\boldsymbol{m}-\boldsymbol{m}_\mathrm{p})$ is the dual function of the indicator function $\psi_K(\boldsymbol{h}_\mathrm{i})$. We can thus write (7) equivalently as

$$\boldsymbol{m} = \arg\max_{\boldsymbol{m}} e(\boldsymbol{m}) - \mu_0\langle \boldsymbol{h},\boldsymbol{m}\rangle + \psi_K^*(\boldsymbol{m}-\boldsymbol{m}_\mathrm{p}), \qquad (19)$$

and the first order optimality condition for this problem is

$$-\left(\tfrac{\partial e}{\partial \boldsymbol{m}}(\boldsymbol{m}) - \boldsymbol{h}\right) = \boldsymbol{h}_\mathrm{i} \in \partial\psi_K^*(\boldsymbol{m}-\boldsymbol{m}_\mathrm{p}). \qquad (20)$$

Noting that $-\boldsymbol{v} = \boldsymbol{m}-\boldsymbol{m}_\mathrm{p}$ and $\boldsymbol{f} = \boldsymbol{h}_\mathrm{i}$, this exactly amounts to the dual relation (14).

III. Parameter Identification

The standard method to obtain a more realistic model for ferromagnetic materials is to introduce a distribution of pinning force levels χ_i weighted by the volume density ω_i (see, e.g., [1]) with the constraint

$$\sum_{i=1}^{N}\omega_i = 1\,; \quad \omega_i \ge 0\,. \qquad (21)$$

This approach corresponds well to the statistical distribution of the pinning force strengths in ferromagnetic materials. In doing so, we may write

$$\boldsymbol{b} \;=\; \mu_0\left(\boldsymbol{h} + \sum_{i=1}^{N}\omega_i\boldsymbol{m}_i\right) \qquad (22)$$

$$\frac{d}{dt}w(\boldsymbol{b},\boldsymbol{m}) \;=\; \boldsymbol{h}\cdot\dot{\boldsymbol{b}} - \sum_{i=1}^{N}\omega_i\,|\chi_i\dot{\boldsymbol{m}}_i| \qquad (23)$$

and, e.g., (8) transforms to

$$\boldsymbol{h}_{\mathrm{r},i} = \arg\min_{\boldsymbol{u}\in K_i(\boldsymbol{h})} S(\boldsymbol{u}) - \langle \boldsymbol{m}_{\mathrm{p},i},\boldsymbol{u}\rangle, \qquad (24)$$

with

$$K_i(\boldsymbol{h}) = \{\boldsymbol{u} : |\boldsymbol{u}-\boldsymbol{h}| \le \chi_i\}\,. \qquad (25)$$

Following [2], we express the anhysteretic curve via

$$M_\mathrm{an}(h_\mathrm{r}) = \frac{2m_\mathrm{s}}{\pi}\mathrm{atan}\frac{h_\mathrm{r}}{A} \qquad (26)$$

with m_s the saturation magnetization and the parameter A determining the steepness of the curve. In doing so, the magnetization $\boldsymbol{m}$ in the composite model computes by

$$\boldsymbol{m} = \sum_{i=1}^{N}\omega_i M_\mathrm{an}(h_\mathrm{r})\frac{\boldsymbol{h}_{\mathrm{r},i}}{h_{\mathrm{r},i}}\,. \qquad (27)$$

The parameter identification is based on Epstein frame measurements of isotropic steel sheets. The excitation coils are loaded by a triangular signal with 1 Hz frequency and decaying amplitude towards zero. The low frequency is chosen to minimize eddy current effects, which should not enter measurements of the BH-curves, since these effects are modeled by the additional eddy current density term within the partial differential equation. The measured BH-curves are displayed in Fig. 1. Now, we assume $N = 31$ possible χ_i values being uniformly distributed between zero and the maximal measured magnetic field intensity $H_\mathrm{max,meas}$ and define the design parameter vector by the steepness A of the anhysteretic curve and the volume densities ω_i

$$\boldsymbol{p} = (A,\,\omega_1,\,\omega_2\ldots\omega_N)^T\,. \qquad (28)$$

The constraint optimization reads as

$$\min\; f(\boldsymbol{p}) = \sum_{k=1}^{M}||\boldsymbol{m}_k - \boldsymbol{m}_{\mathrm{meas},k}||_2^2 \qquad (29)$$
$$\text{s.t.}\; \sum_{i=1}^{N}w_i = 1\,;\; w_i \ge 0\,.$$

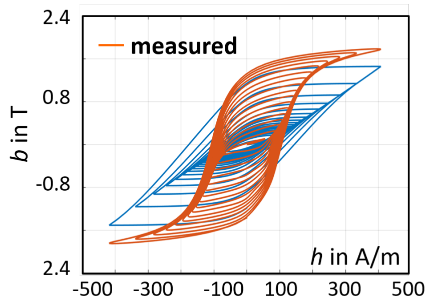

(a) Initial parameters

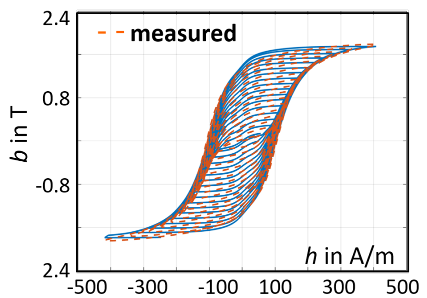

(b) Optimized parameters

Fig. 1: Fitted hysteresis with initial and optimized weights.

For performing the optimization, we used the Matlab function *fmincon* with the following details:

- initial steepness A parameter is 60
- number N of possible χ_i values, which are the pinning forces, is set to 31
- all weights ω_i for the χ_i values are set to $1/31$
- sequential quadratic programming algorithm.

With these chosen initial values, the hysteresis curves have the shape as displayed in Fig. 1a. After 25 iterations, the obtained parameters resulted in hysteresis curves as displayed in Fig. 1b compared to the measured ones. Thereby, the steepness

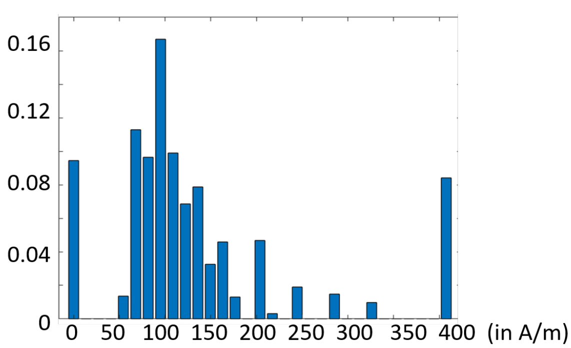

Fig. 2: Optimized volume densities for the different pinning force levels.

parameter changed from 60 to 27.3 and the weights ω_i for the individual pinning force levels are displayed in Fig. 2. One can observe that out from the chosen $N = 31$ values, just 17 are different from zero, which strongly decreases the evaluation time of the hysteresis operator.

IV. Finite Element Formulation

The energy based vector hysteresis model according to [4] has been implemented for the scalar magnetic potential formulation

$$\mathcal{F}(\psi) = -\boldsymbol{\nabla} \cdot (\mu_0 \boldsymbol{\nabla} \psi + \mathcal{P}_{\mathrm{m}}(\boldsymbol{h})) = 0\,, \tag{30}$$

and solved by the Finite Element (FE) method. A straight forward procedure to solve for the scalar magnetic potential is to put the hysteresis dependent term $\mathcal{P}_{\mathrm{m}}(\boldsymbol{h})$ to the right hand side and apply the FE method. Therewith, one arrives at a fixed-point method for the nonlinear system of equations. However, convergence can only be guaranteed when very small incremental steps are made within the nonlinear iteration process. Therefore, we have applied a quasi Newton scheme with a numerically computed Jacobian matrix. In doing so, we may formally write the Newton scheme as follows

$$\mathcal{J}(\underline{\psi}_k)\Delta\underline{\psi} \;=\; -\mathcal{F}(\underline{\psi}_k) \tag{31}$$

$$\underline{\psi}_{k+1} \;=\; \underline{\psi}_k + \Delta\underline{\psi} \tag{32}$$

with the FE solution vector $\underline{\psi}_{k+1}$ at iteration $k+1$. The Jacobian $\mathcal{J}$ is computed via the Davidon–Fletcher–Powell (DFP) formula, which preserve symmetry and positive definiteness and turns the Newton method to a quasi-Newton scheme. In doing so, the approximate Jacobian computes by [6]

$$\mathcal{J} \;=\; \left(\boldsymbol{I} - \frac{\Delta\mathcal{F}_k \Delta\underline{\psi}_k^T}{\Delta\mathcal{F}_k^T \Delta\underline{\psi}_k}\right) \mathcal{J}_k \left(\boldsymbol{I} - \frac{\Delta\underline{\psi}_k \Delta\mathcal{F}_k^T}{\Delta\mathcal{F}_k^T \Delta\underline{\psi}_k}\right) + \frac{\Delta\mathcal{F}_k \Delta\mathcal{F}_k^T}{\Delta\mathcal{F}_k^T \Delta\underline{\psi}_k} \tag{33}$$

$$\Delta\mathcal{F}_k \;=\; \Delta\mathcal{F}_k - \Delta\mathcal{F}_{k-1} \tag{34}$$

with $\boldsymbol{I}$ the unit matrix.

V. Numerical Results

To demonstrate the applicability of the EB hysteresis operator and the developed FE formulation for the magnetic scalar potential to rotating magnetic fields, we chose the computational setup as displayed in Fig. 3. At Γ_{D1}, a time

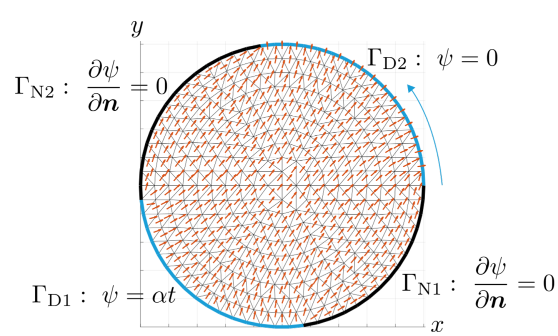

Fig. 3: Computational setup with vector plots of the magnetic field.

increasing magnetic scalar potential is prescribed, whereas at the opposite boundary Γ_{D2} the magnetic scalar potential is set to zero. Furthermore, at the two boundaries Γ_{N1} and Γ_{N1} homogeneous Neumann boundary conditions are set. By rotating the boundaries, as displayed in Fig. 3, a rotating magnetic field is generated, which makes this computational setup an ideal test case for vector hysteresis models. Figure

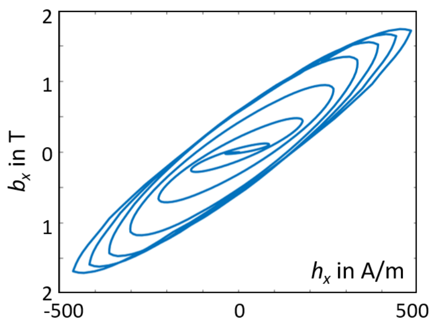

(a) Hysteresis in x-direction

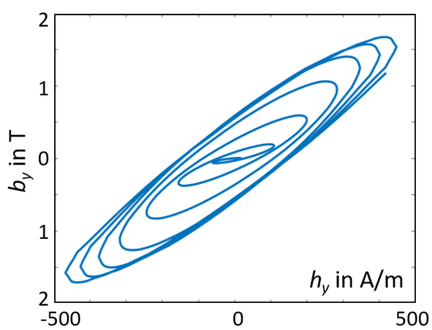

(b) Hysteresis in y-direction

Fig. 4: Hysteresis curves for a characteristic finite element in the computational domain.

4 displays the BH-curves for a characteristic finite element both for the x- as well as y-direction. The evaluation of the hysteresis operators for each finite element takes 2 to 3 iterations and the quasi-Newton scheme needs in average over all computational time steps about 10 iterations. The total computational mesh consisted of 606 triangular elements and for each element a hysteresis operator has been evaluated in its center. The total elapsed computational time for the 435 time steps was $450\,\mathrm{s}$ on one Intel Xeon Gold 5218 CPU core with a maximum clock rate of 3.9GHz. In our numerical tests this efficiency was not dependent on the time step size, and we want to point out that the current implementation is by far not optimized.

Finally, we want to summarize the main advantages of the EB hysteresis model:

- The EB hysteresis model is inherently a vector hysteresis model.
- The formulation is variational consistent, so that all internal variables follow from the minimization of a thermodynamic potential has been proposed.
- The evaluation of the hysteresis operator is performed via the solution of an optimization problem with a very efficient Newton scheme.

VI. Conclusion

Energy based (EB) vector hysteresis models are based on the dry friction model as used in mechanical engineering. Based on the derivations in [5], there are two basic formulations: (1) finding the velocity being the sub-differential of the indicator function dependent on the force; (2) finding the force being the sub-differential of the indicator function dependent on the velocity. In doing so, the second indicator function is exactly the Legendre-Fenchel conjugate function of the first one. Thereby, we could show that the formulation presented in [4] corresponds to the first case and the one published in [3] to the second case. Next, we discussed our parameter identification scheme for the EB hysteresis operator and demonstrated that Epstein frame measurements of hysteresis curves excited by a decaying triangular loading current provides sensitive data to fit the parameters of the hysteresis operator. Thereby, the steepness of the anhysteretic curve and the volume densities for the pinning force levels have composed the design parameter vector in the optimization process based on the sequential quadratic programming algorithm. The FE implementation based on the quasi-Newton method with computing the Jacobian via the Davidon–Fletcher–Powell formula showed good performance for our test case of a rotating magnetic field. Currently, we extend the quasi-Newton scheme by a line search for the update to further reduce the necessary number of iterations per time step.

References

[1] F. Henrotte and A. Nicolet, K. Hameyer, *An energy-based vector hysteresis model for ferromagnetic materials*, COMPEL: The International Journal for Computation and Mathematics in Electrical and Electronic Engineering **25** (2006), no. 1, 71-80

[2] A. Bergqvist, *Magnetic vector hysteresis model with dry friction-like pinning*, Physica B: Condensed Matter **233** (1997), no. 4, 342–347.

[3] V. François-Lavet, F. Henrotte, L. Stainier, L. Noels, and C. Geuzaine. An energy-based variational model of ferromagnetic hysteresis for finite element computations. *J. Comput. Appl. Math.*, vol. 246, pp. 243–250, 2013.

[4] L. Prigozhin1, V. Sokolovsky, J. W. Barrett, and S. E. Zirka. On the energy-based variational Model for vector magnetic hysteresis. *IEEE Trans. Magn.*, vol. 52, pp. 7301211, 2016.

[5] J. J. Moreau. Application of convex analysis to the treatment of elastoplastic systems. in *Applications of Methods of Functional Analysis to Problems in Mechanics (Lecture Notes in Mathematics)*, vol. 503, P. Germain and B. Nayroles, Eds. Berlin, Germany: Springer-Verlag, 1976, pp. 56–89.

[6] R. Fletcher. *Practical Methods of Optimization*. Wiley-Interscience, New York, 1987.